Isı Bilimi ve Tekniği Dergisi, 37, 2, 1-12, 2017
J. of Thermal Science and Technology

ISSN 1300-3615

HEAT TRANSFER FROM AN OSCILLATED VERTICAL ANNULAR FLUID COLUMN THROUGH A POROUS DOMAIN: A THERMODYNAMIC ANALYSIS OF THE EXPERIMENTAL RESULTS

Ersin SAYAR
Istanbul Technical University, Department of Mechanical Engineering
34437 Beyoğlu, İstanbul, Turkey, ersin.sayar@itu.edu.tr

(Geliş Tarihi: 30.06.2016, Kabul Tarihi: 26.12.2016)

Abstract: Heat transfer in an oscillating vertical annular fluid column flowing through a porous domain in the single phase or bubbly flow two-phase regime (sub-cooled or saturated nucleate flow boiling) are investigated experimentally and theoretically, in quasi-steady state conditions. Forced oscillations are applied to water via a frequency controlled dc motor and a piston-cylinder device. Heat transfer is from the stationary concentric tubular electric heating element outer surface to the reciprocating flow. The heat transfer in an oscillating vertical annular fluid column flowing in the single phase or in the bubbly flow regime is altered by using stainless steel wool porous medium. For the single phase region of flow, it is understood that, the effective heat transfer mechanism is enhanced and it is due to the hydrodynamic boundary layer which can not follow the core flow. Bubbly (nucleate) flow boiling in oscillating flow is also investigated experimentally and theoretically using a simplified thermodynamic analysis. The onset of boiling temperature is distinctly dropped compared to the pool and flow boiling experiments on polished surfaces due the finned surface effect of the steel porous domain, due to the enhanced mixing of the boundary layer flow and core flow; due to the improvement of apparent surface roughness and due to the alteration of ebullition cycle (bubbles are limited by the cell volume here). The developed correlation predicted cycle-space averaged Nusselt number is shown to be in good agreement with the experimental data. The present investigation has possible applications in moderate sized wicked heat pipes, boilers, compact heat exchangers and steam generators.
Keywords: Oscillating, Heat transfer experiment, Single phase, Boiling, Sub-cooled, Flow boiling, Porous, Annular duct.

GÖZENEKLİ ORTAMDA DİKEY SALINIMLI HALKASAL BİR AKIŞKAN KOLONUNDAN ISI GEÇİŞİ: DENEY SONUÇLARININ TERMODİNAMİK ANALİZİ

Özet: Bu çalışmada gözenekli ortamda bulunan, salınımlı olarak dikey yönde hareket ettirilen, halkasal bir akışkan kolonunda tek fazlı veya iki fazlı habbecikli akışlı ısı geçişi sanki-sürekli durumda, teorik ve deneysel olarak incelenmiştir. Zorlanmış salınımlar suya DC motor ve piston-silindir aracılığıyla uygulanmıştır. Isı geçişi merkezdeki sabit elektrikli ısıtma elemanından salınımlı akışa olmaktadır. Tek fazlı veya iki fazlı akış rejimindeki salınımlı halkasal akıştan ısı geçişi paslanmaz çelik yün gözenekli ortam vasıtasıyla değiştirilmektedir. Tek fazlı akış bölgesinde oluşan hidrodinamik sınır tabakasının merkezdeki akışı takip edemediği için ısı geçişini iyileştirdiği tespit edilmiştir. Basitleştirilmiş bir termodinamik analiz kullanılarak salınımlı akışta habbecikli (kabarcıklı) akış kaynaması da teorik ve deneysel olarak incelenmiştir. Gözenekli ortamın sebep olduğu kanat etkileri; akıştaki sınır tabakalarının karışımı; efektif yüzey pürüzlülüğünün artışı ve habbelerin büyüklüklerinin gözenekli ortam hücre hacmiyle kısıtlı olması gibi kaynama döngüsü değişiklikleri sebebiyle kaynama başlangıcı sıcaklığının parlatılmış metal yüzey üzerindeki havuz kaynaması ve kaynamalı akışa nazaran kaydadeğer derecede düştüğü tespit edilmiştir. Çevrim ortalama Nusselt sayısı için bir korelasyon geliştirilmiş, ve korelasyonun deney sonuçları ile uyumlu olduğu görülmüştür. Kazanlar, kompakt ısı değiştiricileri, ısı boruları ve buhar jeneratörleri yapılan çalışmanın uygulama alanları içerisindedir.
Anahtar kelimeler: Salınım, Isı geçişi deneyi, Tek faz, Kaynama, Kaynamalı akış, Gözenek, Halkasal boru.

NOMENCLATURE

A	Cross-sectional area of water column (m^2)
A_o	Dimensionless oscillation amplitude
A_p	Cross-sectional area of piston (m^2)
d	Hydraulic diameter of test duct (m)
h	Heat transfer coefficient (W/m^2-K)
H_1, H_2	Cycle-averaged enthalpies in Equation 6 (J)
i	Enthalpy (J/kg)
i_{lv}	Enthalpy of vaporization (J/kg)

Ja	Jakob number
L	Distance from probe 1 to probe 2 (m)
l_h	Heater length (m)
l_o	Distance from probes to heater (m)
Nu_L	Space and cycle averaged Nusselt number
Pr	Prandtl Number
R_{men}	The radius of the liquid-vapor meniscus (m)
Q_{loss}	Total heat loss to environment over a cycle (J)
Q_l	Total heat transferred to water over a cycle (J)
q_e	Total wall heat transfer (W)
q_1"	Heat flux from heater to control volume (W/m^2)
q_2"	Heat flux from insulation layer to environment (W/m^2)
R	Flywheel radius (m)
R_b	Hemispherical vapor bubble effective radius (m)
Re_ω	Kinetic Reynolds number
r	Radial coordinate (m)
r_1	Inner radius of annulus (m)
r_2	Outer radius of annulus (m)
t	Time (s)
T	Temperature
T_0	Average temperature defined in Equation 18 (°C)
T_{10}	First probe temperatures (°C)
T_{20}	Second probe temperatures (°C)
T_a	Ambient temperature (°C)
T_v	The temperature of the vapor adjacent to the meniscus (°C)
T_w	Wall temperature (°C)
T_{wo}	Space-cycle averaged wall temperatures (°C)
u_{AMP}	Amplitude of Darcy velocity (m/s)
u_D	Local Darcy mean velocity (m/s)
y	Vertical coordinate (the origin is at the bottom of the test set-up, $y=y^+$+1.0 m)
y*	Distance from reference to the meniscus (m)
y^+	Vertical coordinate (the origin is at the probe 1)
y_m	Amplitude of oscillations (m)
y_i	Interface position (m)
y_0	Oscillation axis or filling height (m)

Greek Symbols

ε	Volumetric porosity (m^3 fluid volume/m^3 total volume)
δ	Momentum boundary layer thickness (m)
σ	Surface tension (N/m)
ρ	Fluid density (kg/m^3)
ω	Angular frequency (rad/s)
ΔT_{crit}	Critical superheat for bubble formation (°C)

Subscripts

l	Liquid
v	Vapor

INTRODUCTION

Oscillating flows have been a common topic of fundamental investigations in the fields of heat and mass transfer in the recent years. Loop heat pipe (LHP) is a promising application of oscillating flow. LHP is an exceptionally efficient heat transfer device (Wang et al., 2013; Wan et al., 2012). A series of experiments were performed to investigate heat transfer under varying length and inner diameter miniature oscillating heat pipes by Lin et al.(2011). Heat transfer in an oscillating loop heat pipe consisting of three interconnected columns was investigated experimentally by Ozdemir (2007) and also by Arslan and Ozdemir(2008). Chatwin (1975) and Watson (1983) discussed mass transfer in pulsating and oscillating flow, to investigate transport phenomena in organs of the human body. Zhao and Cheng (1998) gave a literature survey on the heat and mass transfer in pulsating and oscillating flow. Kurzweg (1984) investigated the longitudinal heat transfer process. Ozawa and Kawamoto (1991) investigated the heat transfer mechanism experimentally and numerically. The researchers concentrated on the flow of the boundary and bulk regions of the fluid. Zhao and Cheng (1995) carried out a study for forced convection in a long heated pipe subjected to uniform heat flux with a laminar reciprocating flow of air. In another numerical study, Zhao and Cheng (1996) investigated the heat transfer for laminar forced convection of a periodically reversing flow in a pipe heated at constant temperature. Four similarity parameters such as Prandtl number, kinetic Reynolds number, dimensionless oscillation amplitude and the length to diameter ratio of the heated tube were used in their study. Xiaoguo and Cheng (1993) obtained a correlation equation for cycle-averaged Nusselt number in terms of Reynolds number, kinetic Reynolds number and dimensionless fluid displacement. The heat transfer from a vertical wall near an oscillating gas/liquid interface was investigated experimentally by Chen and Chen (1998). An empirical equation for average Nusselt number was recommended. The equation was based on Reynolds number and Prandtl number in the case of oscillating interface without evaporation. Heat transfer from a surface having constant heat flux subjected to oscillating flow in a vertical annular liquid column was investigated experimentally by Akdag and Ozguc (2009). The working fluid was liquid water and the experimental system was open to surrounding atmosphere. Heat removal from the cold surface due to the oscillating liquid column was determined in terms of Nusselt number (Akdag et al., 2008).

The heat transfer mode of boiling in porous media is similar to boiling in wicked surfaces except that evaporation on the top of the porous medium does not have much effect on the formation and growth of the vapor bubbles (Sondergeld, and Turcotte, 1997). Udell (1985) observed boiling in porous media with heat application from above. The vapor bubbles cannot escape from the top of the porous medium as they can in the case of boiling on a wicked surface (Ramesh and Torrence, 1990). Costello and Redeker (1963) investigated the ability of wicking material to adequately supply coolant to a surface in order to sustain boiling. When boiling begins in a fluid-saturated porous medium heated from below, a two layer system is formed with a

liquid region overlying a two-phase region (Nield and Bejan,2013). Experiments by Sondergeld and Turcotte(1977) and Bau et al.(1982) have shown that the liquid regime temperature profile may be conductive or convective, but the two-phase region is essentially isothermal at the saturation temperature (Faghri and Zhang,2006) . Chuah and Carey (1987) studied boiling in an unconfined layer of small spheres on a chrome-plated copper boiling surface. The effect of the particles on heat flux depends on the characteristics of the particles: glass beads delay the onset of pool boiling heat transfer, while copper beads improve it. A numerical study of boiling with mixed convection in a vertical porous layer was made by Najjari and Nasrallah(2002). A three-dimensional simulation of phase-change heat transfer in an asymmetrically heated channel was carried out by Li et al.(2010). Li and Leong(2011) performed an experimental and numerical study of single and two-phase flow and heat transfer in aluminum foams. Damronglerd and Zhang (2006) studied transient fluid flow and heat transfer in a layer with partial heating and evaporation at the upper surface. In general, the boiling characteristics from porous coated surfaces are generally superior when compared to the pool boiling on plain surfaces(Li and Peterson, 2007). The mechanisms of improvement are essentially due to the increase of the wetted area, the number of nucleation sites, the enhanced interaction among bubbles, as well as possible film and capillary evaporation induced through the use of porous coatings. For discussion of some wider aspects of boiling and two-phase flow in porous media, the reader is referred to the reviews by Dhir(Dhir, 1994; Dhir, 1998; Dhir and Cotton,1977;Naik and Dhir 1982). Lipinski(1982) presents a comprehensive review of phase change and two-phase flow phenomena in porous media. Porous coatings with higher thermal conductivity were claimed to perform better than those with lower thermal conductivities, especially at low heat fluxes. Accordingly, different from previous studies the motivation of the present study is to investigate single phase heat transfer and two-phase boiling performance of water in a moderate thermal conductivity (stainless steel, k = 15 W/mK) porous domain where the experimental test section is annular. Enhanced boiling surface may affect boiling characteristics; lowering the temperature at onset of nucleate boiling; improving the heat transfer coefficient in the nucleate boiling regime; increasing the critical heat flux(Furberg, 2011). Lowering the temperature at onset of nucleate boiling indicates that the boiling heat transfer in porous layers occurs within a narrower range of wall superheat and, hence, may be more suitable for applications where precise temperature control is required. The present study primarily focuses and covers the relationship of enhanced surface/volume features and the related heat transfer mechanisms of the nucleate boiling regime in a porous domain. This study reports part of an extensive experimental research on the heat transfer from a surface heated with constant heat flux to an oscillating vertical annular water column. The analysis is carried out for three different oscillation frequencies and four applied wall heat fluxes while the displacement amplitude and the thermo-physical – material properties of the stainless steel wool porous medium can assumed to be constant for all the cases considered. In the experiments, the heated surface temperature is varied as a result of the amount of electrical power supplied. Power is set to produce four discrete wall heat fluxes and three different frequencies of the forced oscillations are controlled by the external piston-cylinder device. A correlation equation is obtained for the cycle-averaged Nusselt number as a function of kinetic Reynolds number and Jakob number. Annular oscillating water column is driven through a stainless steel wool porous media in order to mix the liquid and vapor phases and hence enhance the hydrodynamic and thermal performance of the system. As opposed to the all the reported works at the best of the authors knowledge, the present study investigates the oscillating flow in an annulus for the first time where the evaporation and boiling are significant (in other words, the closest study, to the present one is Chen and Chen (1998) investigates for oscillating interface without evaporation).

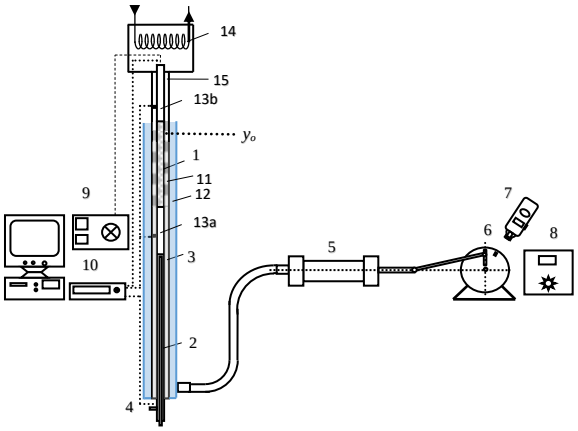

Figure 1 : Experimental setup, 1 Heater, 2 Cooler, 3 Glass pipe, 4 Cooling water inlet and outlet, 5 Piston cylinder apparatus, 6 DC Motor, 7 Digital tachometer, 8 Velocity control, 9 Power supply, 10 Data acquisition system (Keithley-2700), 11 Stainless steel wool porous domain 12 Thermal insulation 13 Teflon parts (a) and (b) 14 Water vapor condenser and 15 Piezoresistive transmitter.

EXPERIMENTAL SETUP

Figure 1 is a schematic diagram of the experimental setup. The outer part of the vertical annular test section is made of tempered glass which is 2.0 m in length, 37.5 mm in inner diameter and 42.0 mm in outer diameter. A layer of thermal insulation (Polyethylene pipe insulation, 0.034 W/mK) is applied to the exterior of the tempered glass test section. The inner and exterior diameters of the insulator are 42.0 mm and 65.0 mm, respectively. A cylinder 18.0 mm in outer diameter consisting of four zones (from top to the bottom: adiabatic (a), heater, adiabatic (b), cooler parts) is anchored precisely and

located at the centerline of the glass tube using three in-house manufactured small positioners. The positioners are located sufficiently far enough from the cooler and heater sections so that they do not significantly disturb the flow or heat transfer. Accordingly, the annuli that the working fluid occupies has inner diameter 18.0 mm and outer diameter 37.4 mm. The heater and cooler are made of concentric copper tubes with lengths of 600.0 and 760.0 mm, respectively. The adiabatic teflon parts (both (a) and (b)) are 300.0 mm in length. One of the adiabatic parts is located between the heater and cooler. The other adiabatic part is screwed smoothly to the top of the heater. The top adiabatic part is in the shape of a hollow tube in order to house the cables of the heater. The axial heat conduction in the teflon cylinder and teflon hollow tube are negligible compared with the copper ones. These four zones are assembled together using threaded joints in order to obtain smooth continuous surfaces among the consecutive sections.

The heater is built by embedding electric resistance wires inside a copper tube. Five thermocouple wires located at the inside of the heater tube are taken out of the test section by passing them through the inside of the heater tube and the adiabatic hollow teflon tube. DC power is used to feed the heater in order to prevent thermocouples from electrical inductance. This is a precaution just because the thermocouple cables are located close to the electrical cables in the heater section. Using five other thermocouple wires, surface temperature of the electrical heater is also recorded. The cooler is made of two concentric copper tubes. The cooling water enters the inner tube which is 6.0 mm / 8.0 mm in inner/outer diameter and leaves from the 16.0 mm / 18.0 mm inner/outer diameter outer tube of the cooler. Seven thermocouples are welded on the cooler surface and the leads are taken out of the test section by passing them through the cooling water.

The heat transfer in an oscillating vertical annular fluid column flowing in the bubbly flow regime is altered by using stainless steel wool (comprises off open-cell, discrete porous cells interconnected to each other geometrically and through a possible contact resistance) which produces a homogeneous porous medium within the system. The porous media has a moderate thermal conductivity (k = 15 W/mK). Porosity, ε (void fraction) of the porous domain is 93.75 % for the volume swept by the oscillating flow and porosity for the entire porous domain is 93.69 %. Accordingly, the porous domain is claimed to be distributed homogenously along the length of the electrical heater.

The thermocouples are placed such that they do not alter the fluid flow i.e. they are placed inside the cooler, heater sections or on the outer surface of the glass tube and insulation layer. There are two thermocouple bundles positioned inside the working fluids and they are called ‘probes’ in the present study. The first temperature probe is located at the half way of the adiabatic section between heater and cooler in order to measure the variation of water temperature with radius (r). The first temperature probe location is also the reference position to measure the vertical positions of the surface temperatures and the interface. This first probe consists of four thermocouples located at different radial positions across the same elevation (constant y) of the annular gap. The second probe is similar to the first one but it is positioned at 150.0 mm above the heater section. Each thermocouple signal of the probes is recorded and then the probe temperatures are calculated by area-weighted averaging of the thermocouple data over the cross-sectional area.

The outer surface temperatures of the glass tube are also measured by ten thermocouples. The outer surface temperatures of the pipe exterior insulation are also measured by additional six thermocouples. All thermocouples are calibrated using a constant temperature bath before the experiments. The thermocouples are Omega K-type Nickel-Chromium vs. Nickel-Aluminum with a diameter 0.6 mm.

The pressure at the water vapor condenser is measured by Keller model PAA-23 piezoresistive transmitter. The transmitter was calibrated by the manufacturer. The transmitter is able to measure absolute pressure up to 1.0 bar. The transmitter is connected to a data acquisition system. The transmitter provide 0–10 V electric potential signals, which are converted to actual pressure values using a linear relation between voltage and pressure.

A computer controlled data acquisition system (Keithley 2700) is used to collect temperature, pressure, electrical potential and current data. The reciprocating motion of the water column is generated using a piston-cylinder driven by a 1 kW DC motor with adjustable speed and a piston-cylinder device. The number of revolutions of the motor is measured by an optical digital tachometer (Lutron DT-2234B). The filling height of the water column is kept constant for all the cases (y_0=625 mm). The experiments are conducted at for four different heating powers and three different actuation frequencies.

Uncertainity Analysis

Using the measurable quantities (electric potential, current, temperature and diameter) main error sources were investigated. Applied heat is determined by the product of voltage and current, which are measured with the accuracy of 2 % and 1 %. The temperature values are obtained by thermocouples of 1 ℃ accuracy, and for each case, 500 values are collected from each thermocouple, when the system is in pseudo-steady state condition. The diameters were measured using a digital caliper with the accuracy of +/-0.03 mm. To ensure if the system is in the pseudo-steady state, temperatures of every 20 minutes are compared, and decision of pseudo-steady state condition is made by obtaining the relative convergence below 1%. It takes up to 6 hours for each experiments to reach pseudo-steady state.

MATHEMATICAL MODEL

The Critical Superheat for Bubble Formation in Porous Domain

A surface coated with a porous layer is named a wicked surface in Faghri and Zhang(2006). Some vapor nuclei can always exist within the porous structure, but the superheat is essential for these bubbles to grow. The critical superheat for bubble formation in porous domain given in Faghri and Zhang(2006 is summarized here. Critical superheat for bubble formation in a porous domain is obtained as Faghri(1995):

$$\Delta T_{crit} = T_w - T_v = \frac{2\sigma T_v}{i_{lv}\rho_v}\left(\frac{1}{R_b} - \frac{1}{R_{men}}\right) \quad (1)$$

which indicates that the required superheat in a porous surface is lower than that for a plain surface.

Working Fluid Velocity

The amplitude of Darcy velocity of the water column is:

$$R\omega A_p/(A\varepsilon) = u_{AMP}$$

where Ap is the piston cross-sectional area, A is the water column cross-sectional area, R is the flywheel radius and ω is the actuation frequency. The temporal variation of the Local Darcy mean velocity can be written as follows:

$$u_D(t) = u_{AMP}\cos\omega t \quad (3)$$

It can be assumed that the interface is a flat surface once the capillarity and wall effects are neglected. The height yi(t) (represents the approximate position of the interface) can be derived via integration of Equation (3):

$$y_i(t) = y_0 + \frac{RA_p}{A\varepsilon}\sin\theta = y_0 + y_m\sin\omega t \quad (4)$$

Here, $y_m = RA_p/(A\varepsilon)$ is the amplitude of oscillations and y_0 is the oscillation axis or similarly the initial filling height (both are shown in Figure 2). It is also found that the piston-cylinder device driving motor frequency measured by tachometer is identical to the frequency of the recorded interface motion. The frequency of the recorded interface motion is calculated using the Tracker video analysis and modeling tool (a software developed by Open Source Physics). The Fast Fourier Transform analysis (results are not shown here for brevity) of the measured temperature data points out the same base frequency with some small kinks at various other frequencies.

Calculation Method of the Cycle-Averaged Heat Transfer

A typical length scale has an order of $\sqrt{2\nu/\omega}$ for the region that inertial and viscous forces in the flow domain are comparable. The momentum diffusion decreases quickly away from the wall and the porous domain. Accordingly, the penetration depth (the depth where the wall effects are in action) is approximately given by Zhao and Cheng (1998) as follows:

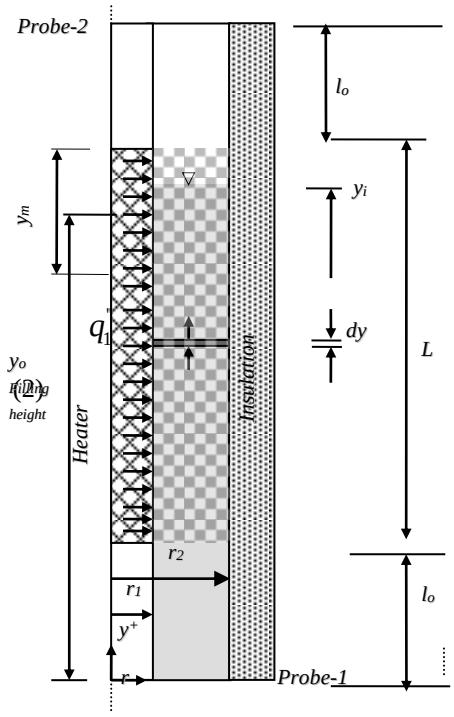

Figure 2. Control volume for the mass, energy and momentum conservation equations

$$\delta \cong 3\sqrt{2\nu/\omega} \quad (5)$$

This depth is below 1 mm for the frequencies considered in the present study. Thus, the velocity profile can be assumed uniform in the annular channel.

The conservation equations of mass, momentum and energy can be solved for the fluid, porous media and the solid matrix in a coupled algorithm within the system undergoing periodic compression and expansion. Convective heat transfer source term representing the heat transfer from the solid matrix to the fluid should be included in the energy conservation equations for the fluid and for the solid matrix as well. Viscous loss (includes Darcy permeability) and inertial loss (includes Forchheimer number) terms alter the momentum

equation for the porous media zones. Further discussion and solution of the listed governing equations are beyond the scope of the present experimental investigation and that can be conducted in future studies.

Interface position y+ approximately indicates the position of the water–vapor interface in this conjugate heat transfer problem of the water–vapor system. The water–vapor interface is not a flat surface because of the capillary and the water film created by the motion. Thus, the wetted heater surface cannot satisfactorily be identified only by the y+-position. Consideration of the thermal energy for water and vapor regions individually does not give practical results, due to the fact that the shape of the interface surface and the velocity at each point along the interface are presently unknown. Accordingly, the thermal energy equation for the entire system consisting of both water and vapor regions is considered. Once energy equation is integrated over the control volume shown in Figure 2, i.e. $y^+ = 0$ to L and also integrated over a cycle in time domain, the following expression is obtained:

$$H_2 - H_1 = q_1^{"} 2\pi r_1 l_h \left(\frac{2\pi}{\omega}\right) - \int_0^{\frac{2\pi}{\omega}} \int_0^L 2\pi r_2 q_2^{"} dy^+ dt \tag{6}$$

where cycle-averaged enthalpies are $H_1 = \int_0^{\frac{2\pi}{\omega}} \varepsilon u_D A \rho_l i_{bl}(0,t) dt = \int_0^{\frac{2\pi}{\omega}} \varepsilon u_D A \rho_l c_l T_{bl}(0,t) dt$ (thermal energy of the working entering to the control volume) and $H_2 = \int_0^{\frac{2\pi}{\omega}} u_v A \rho_v i_v(y_i,t) dt$ (thermal energy of the working leaving the control volume). Here $i_v(y_i,t)$ is the enthalpy of the two-phase mixture leaving the control volume and $i_v(y_i,t) \approx i_{lv}$ (with the assumption saturated vapor leaves the system and condense enters back to the control volume at the saturated liquid state). q1",q2" are the heat fluxes on the heater surface and the outer surface of the insulation layer, respectively where q2" can assumed to be zero since the exterior of the system is well-insulated. Equation (13) shows the thermal energy balance of the control volume. Enthalpy difference over the control volume (H2-H1) is equal to the heat transfer at the control volume inner and outer surfaces. The heat input $q_1^{"} 2\pi r_1 l_h \left(\frac{2\pi}{\omega}\right)$, is constant over a cycle during the pseudo-steady state of the experiments. The last term on the right hand side of Equation (6) shows the total heat loss from the exterior of the insulation layer to the surrounding room air over a cycle and it is assumed zero. The heat flux from the insulation outer surface to the environment is not constant; it varies with position and time. However, its magnitude is found to be negligible compared to the other terms in the governing equations. Enthalpy difference over the control volume is rearranged as follows:

$$Q_l = (H_2 - H_1) = q_1^{"} 2\pi r_1 l_h \left(\frac{2\pi}{\omega}\right) - Q_{loss} \tag{7}$$

$$Q_{loss} = \int_0^{\frac{2\pi}{\omega}} \int_0^L 2\pi r_2 q_2^{"} dy^+ dt = 0$$

where . Ql is the total heat transferred to water over a cycle, i.e. the net thermal energy entering to the control volume from the heater. The variation of the measured surface temperatures of the exterior side of insulation with time are neglected according to the observations during the experiments. The surface temperatures of the inner side of the glass tube perhaps vary harmonically with time. Outer surface temperatures have a pretty steady behavior with negligible minor harmonic oscillations which can be attributed to the thermal capacitance effects of the glass wall and exterior insulation layers.

The thermal energy equation for the boiling of two-phase liquid-vapor mixture region over a cycle without flat interface simplification can be written as follows:

$$Q_l = \int_0^{\frac{2\pi}{\omega}} \int_{l_0}^{y^*} 2\pi r_1 q_1^{"} dy^+ dt - \int_0^{\frac{2\pi}{\omega}} \int_0^{y} 2\pi r_2 q_2^{"} dy^+ dt \tag{8}$$

$$\int_0^{\frac{2\pi}{\omega}} \int_0^{y_i} 2\pi r_2 q_2^{"} dy^+ dt$$

where, is assumed zero. Here, y* is the distance from probe-1 to the meniscus. The last term on the right hand side of this equation shows the neglected heat loss from the boiling of two-phase liquid-vapor mixture side of the insulation to the environment, so that the Equation (8) can be rearranged to give the total heat transfer to water from the heater over a cycle as:

$$Q_l = \int_0^{\frac{2\pi}{\omega}} \int_{l_0}^{y^*} 2\pi r_1 q_1^{"} dy^+ dt \approx q_1^{"} 2\pi r_1 l_h \left(\frac{2\pi}{\omega}\right) \approx q_e \left(\frac{2\pi}{\omega}\right) \tag{9}$$

RESULT AND DISCUSSION

Cycle-averaged experimental data are given in the Table 1 with varying actuation frequencies of the piston-cylinder driver motor and the applied electrical heater power for each one of experiments.

Temporal variation of temperatures are given in Figures 3a-d (Table 1: Exp-10, q_e = 180.0W, ω=1.434rad/s, ym = 0.10m, y_0 = 1.625m), respectively for the heater

outer surface (Figure 3a); glass tube external surface (Figure 3b); insulation outer surface (Figure 3c) and Probe-1 (Figure 3d) (Please also see Figures 1 and 2). Total wall heat transfer, qe and angular frequency ω are kept constant for all figures i.e. temperature versus time and vertical coordinate are shown. As shown in Figure 3a, wall temperatures are slightly above the saturation temperature (97.6 °C) of the working fluid. Saturation temperature is calculated as 97.6 °C using the measured absolute averaged pressure of 95 kPa for all conducted experiments. Boiling starts when the temperature of the liquid near the heaters reaches the saturation temperature of the liquid. The superheat at this state is typically less than 1°C, which is much lower than that for the onset of nucleate boiling during pool boiling on a polished surface. The experiments conducted by Sondergeld and Turcotte (1977) revealed that no significant superheat is required to initiate boiling in porous media. In this regime, the heat flux throughout most of the regime is enhanced compared to pool boiling Rannenberg and Beer (1980) and Rudemiller (1989). In Figure 3b glass wall exterior surface temperatures are shown. Between the heater outer surface temperature and the glass outer surface there are two thermal resistances one is due to convection of internal flow and the outer one is due to the conduction resistance through the glass tube. At similar vertical coordinates the difference between heater outer surface temperature and glass tube outer surface temperatures are insignificant which is a direct result of the following physical mechanism. The vapor rises due to buoyant forces, inertia of the reciprocating flow and vapor pressure gradient, and liquid is pulled down to the heater surface by capillary forces, inertia of the reciprocating flow and gravity. Heat transfer that occurs with the counter-filtration of the vapor and water phases is best described as an evaporation/convection/condensation mechanism. In Figure 3c, insulation outer surface temperatures are given. These temperatures are used to check the consistency between the heat conduction through the pipe insulation and convective-radiative heat transfer to the laboratory where heat loss to the room is found negligible compared to the total heat given to the electrical heater. During the experiments the doors and the windows of the room are kept closed and the velocity of air in the room are measured to be below 1.0 m/s. In Figure 3d, temperatures of Probe 1 is plotted at four radial coordinates where four thermocouples are installed radially at the same y position, y=1000.0mm. The radial distribution of temperatures are insignificant due to the enhanced mixing provided by the steel wool porous domain.

The time-averaged heater outer surface; glass tube external surface and insulation outer surface temperatures at various vertical coordinates at three different actuation frequencies are shown in Figures 4a, 4b and 4c, respectively where the experimental conditions are listed as (Table 1: Exp-1-3), q_e = 115.0W, ω=1.434rad/s; 2.079rad/s or 2.273rad/s,y_m = 0.10m, y_0 = 1.625m. The time-averaged heater outer surface temperatures in Figure 4a are approximately linear a typical case for the fully developed flows. The flow through the heating section can be considered fully developed due to the mixing provided by the porous domain. It decreases slightly at y=1506.5 mm vertical position due to the cooling provided by the condensing vapor and by the heat transfer to the environment. The onset of boiling temperature is distinctly dropped compared to the flow boiling experiments on polished surfaces due the finned surface effect of the steel porous domain, due to the enhanced mixing of the boundary layer flow and core flow; due to the improvement off apparent surface roughness and due to the alteration of ebullition cycle (bubbles are limited by the cell volume here). According to the experimental results, bubbles induce highly efficient heat transfer mechanisms. Experimental study proved that the frequency, and wall temperature are important parameters affecting heat transfer. As shown in Figure 4b, time-averaged glass tube outer surface temperatures increase until saturated boiling (i.e. bulk fluid temperature is 97.6 °C) is reached in the test section (corresponding y=1.375m, here), the temperatures decrease close to the top cooling-condensation part (y=1.750m and y=1.925m). Similar trend to the time-averaged glass exterior surface temperatures, exterior surface temperatures of the insulation increases along the heating section then it decreases along the condenser-cooler section.

Time-averaged probe temperatures (Figures 1 and 2) versus applied electrical power at three different actuation frequencies are shown in Figure 5a (Probe-1) and Figure 5b (Probe-2) for all the cases considered. Experimental conditions and the results are tabulated in Table 1 (Exp-1-12, q_e = 115W-180W, ω=1.434rad/s; 2.079rad/s or 2.273rad/s, y_m = 0.10m, , z_0 = 1.625m). For Probe-1 in Figure 5a, at ω=1.434rad/s (actuation frequency of the piston cylinder device) boiling heat transfer is much prominent as it is compared to single phase heat transfer mechanism at q_e=150W and 180.0W. On the other hand, at q_e=115W and 132.5W single phase heat transfer takes over. At ω=2.079rad/s boiling heat transfer is much prominent as it is compared to single phase heat transfer mechanism at q_e=132.5, 150W and 180.0W. On the other hand, at q_e=115W single phase heat transfer takes over. At ω=2.7227rad/s the vapor bubbles are visually observed to exist perhaps the contribution due to two-phase heat transfer at that comparably high frequency is minor therefore at all wall heat fluxes the single phase heat transfer is the dominant one. For the single phase region of flow, it is understood that, the effective heat transfer mechanism is enhanced and it is due to the hydrodynamic boundary layer which can not follow the core flow. In oscillating flow, the heat transfer coefficient is strongly affected for the single phase flow. In Figure 5b, Probe-2 temperatures are shown at four wall heat fluxes and three actuation frequencies. According to the results in Figure 5b, the temperatures within the cooler-condenser section approach to the condensation temperature as the relative strength of boiling increases relative to the single phase heat transfer within the experimental set-up.

Table 1. Cycle averaged experimental data

	ω (rad/s)	q_e (W)	T_{w0} (°C)	T_{20} (°C)	T_{10} (°C)	Re_ω	Ja	h (W/m2K)	Nu_L (exp)	Nu_L (Corr)	Abs.Error (%)
Exp-1	1.43	115.1	97.6	95.9	83.3	1719.0	5.28E-5	421.6	373.9	395.4	5.7
Exp-2	2.08	114.1	93.3	93.0	82.4	2492.2		598.9	531.1	576.5	8.5
Exp-3	2.72	114.6	85.8	85.7	77.4	3263.9		899.6	797.9	754.9	5.4
Exp-4	1.43	132.1	99.6	99.6	85.2	1719.0	3.70E-3	541.2	480.0	479.7	0.1
Exp-5	2.08	132.6	98.5	98.0	86.6	2492.2	1.70E-3	629.2	558.0	545.8	2.2
Exp-6	2.72	132.7	92.6	92.5	83.3	3263.9		867.4	769.3	754.9	1.9
Exp-7	1.43	150.3	99.9	99.8	85.6	1719.0	4.31E-3	615.4	545.8	538.7	1.3
Exp-8	2.08	150.3	99.9	99.7	88.3	2492.2	3.77E-3	792.5	702.9	704.2	0.2
Exp-9	2.72	150.3	97.9	97.4	88.1	3263.9	6.12E-4	860.2	762.9	718.5	5.8
Exp-10	1.43	178.7	100.3	99.8	86.5	1719.0	5.08E-3	735.6	652.4	632.6	3.0
Exp-11	2.08	180.0	100.1	99.8	89.5	2492.2	4.68E-3	975.9	865.5	842.1	2.7
Exp-12	2.72	178.2	100.4	100.3	90.5	3263.9	4.40E-3	1152.1	1021.8	1042.4	2.0

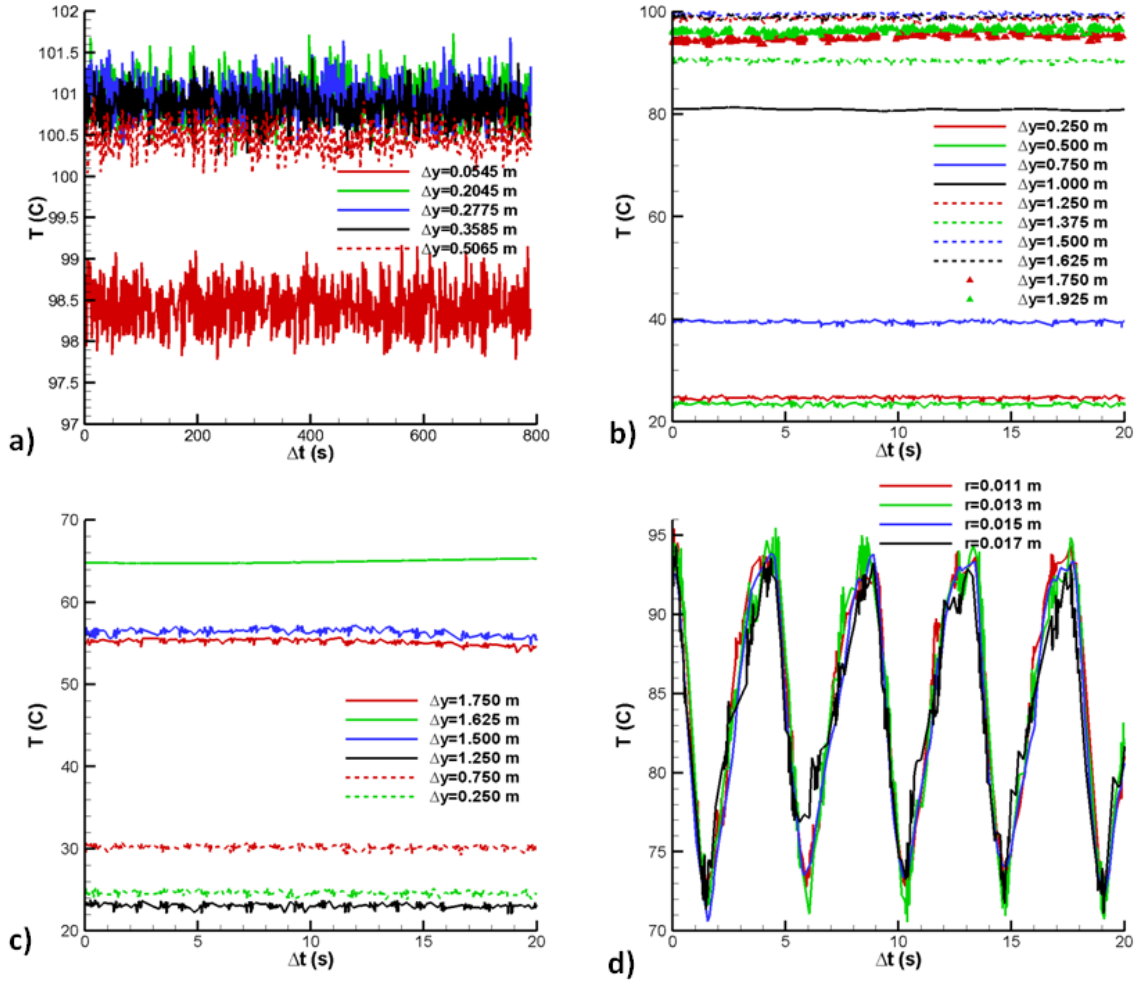

Figure 3. Temperatures versus time (Table 1: Exp-10, q_e = 180.0W, ω=1.434rad/s, y_m = 0.10m, y_0 = 1.625m, Δy, distance from the bottom end of the tubular test section). a) Heater outer surface b) Glass tube external surface c) Insulation outer surface d) Probe-1

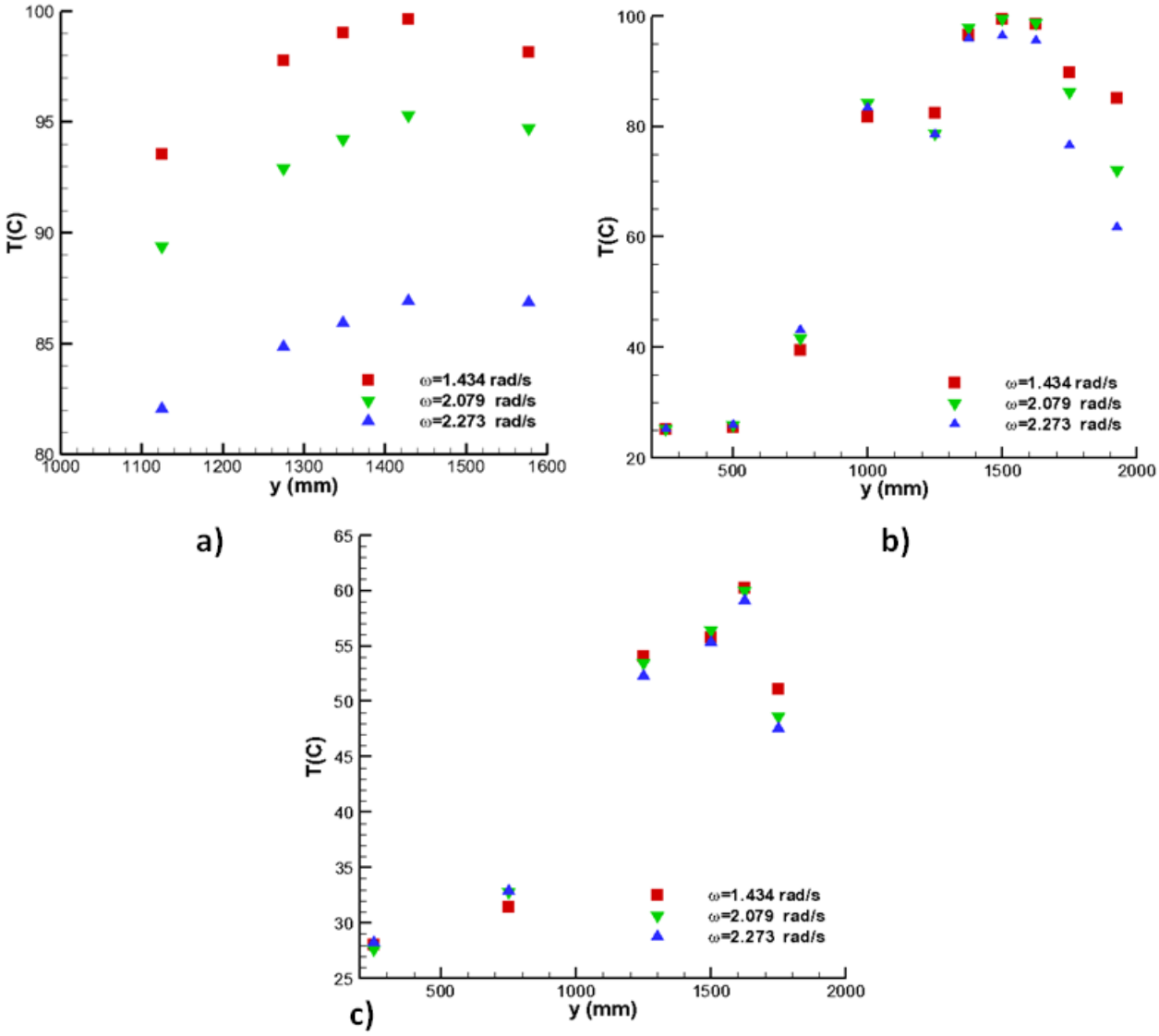

Figure 4. Time-averaged temperatures versus vertical coordinate at three different actuation frequencies (Table 1: Exp-1-3, q_e = 115.0W, ω=1.434rad/s; 2.079rad/s or 2.273rad/s,y_m = 0.10m, y_0 = 1.625m). a) Heater outer surface b) Glass tube external surface c) Insulation outer surface

Prediction of Nusselt Number

The total heat transfer to water from the heater over a cycle Ql can alternatively be written as follows:

$$Q_l = 2\pi r_1 l_h h\left(T_{w0} - T_0\right)(2\pi/\omega) \tag{10}$$

Here, the averaged water temperature can be defined as:

$$T_0 = \frac{T_{10} + T_{20}}{2} \tag{11}$$

T_{10} and T_{20} represent time and space averaged probe temperatures (listed in Table 1). Parallel to the Equation (10), the space and cycle averaged Nusselt number is defined as:

$$Nu_L = \frac{hl_h}{k} = \frac{l_h}{k}\frac{Q_l}{2\pi r_1 l_h (T_{wo} - T_0)(2\pi/\omega)} \tag{12}$$

The calculated Nusselt numbers using Equation (12) are tabulated in Table 1 according to the applied frequencies and heater power. Nusselt number is given as a function of the kinetic Reynolds number $Re_\omega = \omega d^2/\nu$, modified Jakob number,

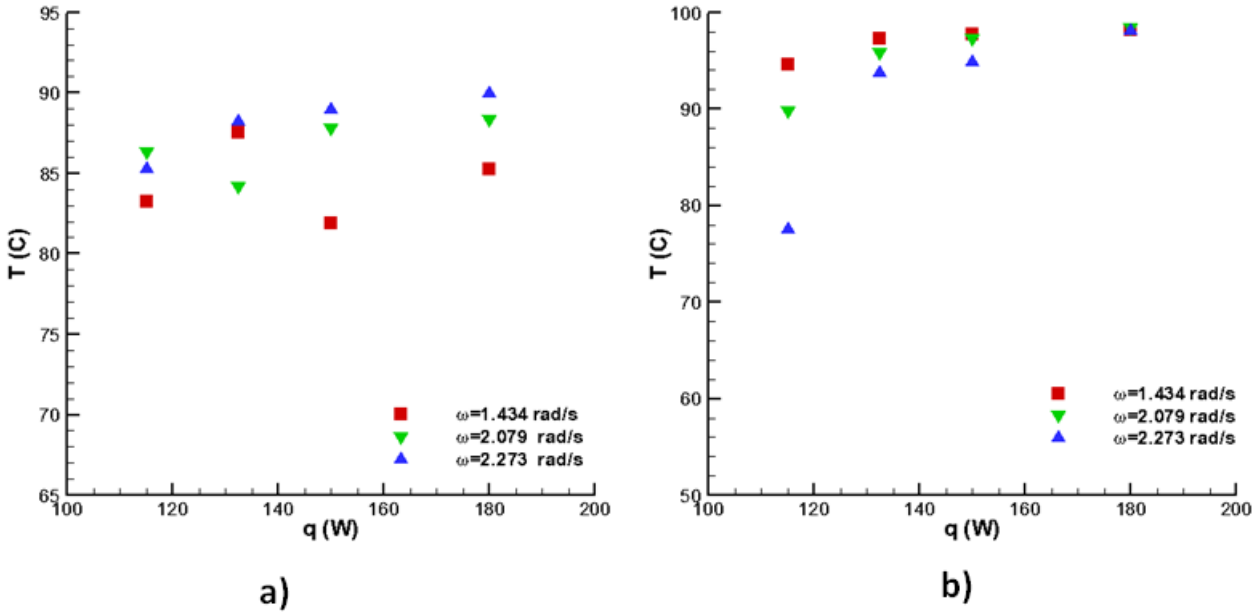

Figure 5. Time-averaged probe temperatures versus applied electrical power at three different actuation frequencies (Table 1: Exp-1-12, q_e = 115W-180W, ω=1.434rad/s; 2.079rad/s or 2.273rad/s, y_m = 0.10m, , y_0 = 1.625m). a) Probe-1 b) Probe-2

$$Ja = \frac{c_{p@T_0}\left[T_{wo} - T_{sat}\right]}{i_{lv}} \qquad (14)$$

dimensionless oscillation amplitude $A_o=2x_m/d$, the aspect (hydraulic diameter to length) ratio of the heater d/lh and Prandtl number as Zhao and Cheng(1995) :

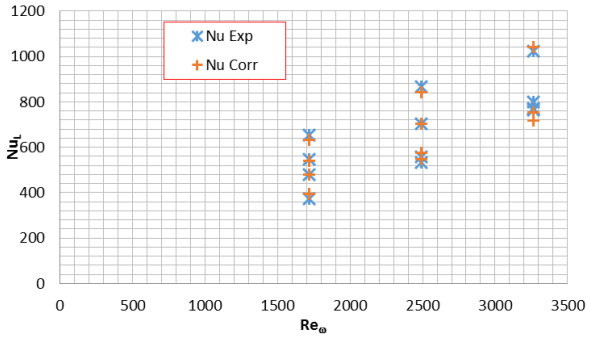

Figure 6. Nusselt number versus kinetic Reynolds number

$$Nu_L = f(Re\omega, Ja, A_0, d/l_h, Pr) \qquad (14)$$

In this study, the parameters A_0, d/l_h, Pr are kept constant while the kinetic Reynolds number and Jakob number are varied. The correlation equation for Nusselt number is found using the non-linear regression analysis as:

$$Nu_L = \left(10116Ja^2 - 23.408Ja + 0.2306\right)\mathrm{Re}_\omega \qquad (15)$$

The coefficient of determination is $R^2 = 0.9787$ and the given correlation is applicable in the following range of kinetic Reynolds numbers according to the the present experiments.

$$1700<Re\omega<3300$$

The graphical representation of Equation (15) is shown in Figure 6 together with the experimental data.

CONCLUSION

Nusselt correlation for the single phase and two-phase heat transfer from a forced oscillated vertical annular fluid column through a porous medium is obtained experimentally. Heat transfer is from a surface heated with constant heat flux to an oscillating single phase or boiling vertical annular water column in the present paper. The inner wall of the stationary concentric element is heated and water is oscillated through the annuli by an external piston-cylinder system. The analysis is carried out for the case of three different oscillation frequencies and four different applied wall heat fluxes while the displacement amplitude remains constant. A control volume formulation is introduced in order to investigate the total heat transfer to water over a cycle. The predicted cycle-space averaged Nusselt number (using the kinetic Reynolds number and Jakob number) is shown to be in good agreement with the experimental data where the coefficient of determination is $R^2 = 0.9787$. The experimental results demonstrated that boiling in porous media could occur over a large range heat flux, i.e., from 0 to 5.3 kW/m2, and at the same time, within a much narrower wall superheat, i.e., <2°C, than for plain surfaces. This indicates that the boiling heat transfer in porous layers occur within a narrower range of wall superheat and, hence, may be more suitable for applications where precise temperature control is required.

REFERANCES

Akdag, U. and A.F. Ozguc, *Experimental investigation of heat transfer in oscillating annular flow.* International Journal of Heat and Mass Transfer, 2009. **52**(11-12): p. 2667-2672.

Akdag, U., M. Ozdemir, and A.F. Ozguc, *Heat removal from oscillating flow in a vertical annular channel.* Heat and Mass Transfer, 2008. **44**(4): p. 393-400.

Arslan, G. and M. Ozdemir, *Correlation to predict heat transfer of an oscillating loop heat pipe consisting of three interconnected columns.* Energy Conversion and Management, 2008. **49**(8): p. 2337-2344.

Bau, H. and K. Torrance, *Low Rayleigh number thermal convection in a vertical cylinder filled with porous materials and heated from below.* Journal of Heat Transfer, 1982. **104**(1): p. 166-172.

Chatwin, P.C., *Longitudinal Dispersion of Passive Contaminant in Oscillatory Flows in Tubes.* Journal of Fluid Mechanics, 1975. **71**(Oct14): p. 513-527.

Chen, Z.D. and J.J.J. Chen, *A simple analysis of heat transfer near an oscillating interface.* Chemical Engineering Science, 1998. **53**(5): p. 947-950.

Chuah, Y. and V. Carey, *Boiling Heat Transfer in a Shallow Fluidized Particulate Bed.* Journal of Heat Transfer, 1987. **109**(1): p. 196-203.

Costello, C. and E. Redeker. *Boiling heat transfer and maximum heat flux for a surface with coolant supplied by capillary wicking*. in *Chem. Eng. Progr. Symposium Ser*. 1963.

Damronglerd, P. and Y. Zhang, *Transient fluid flow and heat transfer in a porous structure with partial heating and evaporation on the upper surface.* Journal of Enhanced Heat Transfer, 2006. **13**(1).

Dhir, D.V.K., *Boiling and two-phase flow in porous media.* Annual review of heat transfer, 1994. **5**(5).

Dhir, V., *Boiling heat transfer.* Annual review of fluid mechanics, 1998. **30**(1): p. 365-401.

Dhir, V. and I. Catton, *Dryout heat fluxes for inductively heated particulate beds.* Journal of Heat Transfer, 1977. **99**(2): p. 250-256.

Faghri, A. and Y. Zhang, *Transport phenomena in multiphase systems*. 2006: Academic press.

Faghri, A. *Heat pipe science and technology*. in *Fuel and Energy Abstracts*. 1995.

Furberg, R., *Enhanced Boiling Heat Transfer on a Dendritic and Micro-Porous Copper Structure.* 2011.

Kurzweg, U.H. and L. Dezhao, *Heat-Transfer by High-Frequency Oscillations - a New Hydrodynamic Technique for Achieving Large Effective Thermal-Conductivities.* Physics of Fluids, 1984. **27**(11): p. 2624-2627.

Li, H., et al., *Three-dimensional numerical simulation of fluid flow with phase change heat transfer in an asymmetrically heated porous channel.* International Journal of Thermal Sciences, 2010. **49**(12): p. 2363-2375.

Li, C. and G. Peterson, *Parametric study of pool boiling on horizontal highly conductive microporous coated surfaces.* Journal of heat transfer, 2007. **129**(11): p. 1465-1475.

Li, H. and K. Leong, *Experimental and numerical study of single and two-phase flow and heat transfer in aluminum foams.* International Journal of Heat and Mass Transfer, 2011. **54**(23): p. 4904-4912.

Lin, Z.R., et al., *Experimental study on effective range of miniature oscillating heat pipes.* Applied Thermal Engineering, 2011. **31**(5): p. 880-886.

Lipinski, R.J., *Model for boiling and dryout in particle beds.[LMFBR]*. 1982, Sandia National Labs., Albuquerque, NM (USA).

Naik, A.S. and V. Dhir, *Forced flow evaporative cooling of a volumetrically heated porous layer.* International Journal of Heat and Mass Transfer, 1982. **25**(4): p. 541-552.

Najjari, M. and S. Ben Nasrallah, *Numerical study of boiling with mixed convection in a vertical porous layer.* International Journal of Thermal Sciences, 2002. **41**(10): p. 913-925.

Nield, D.A. and A. Bejan, *Mechanics of Fluid Flow Through a Porous Medium*. 2013: Springer.

Ozawa, M. and A. Kawamoto, *Lumped-Parameter Modeling of Heat-Transfer Enhanced by Sinusoidal Motion of Fluid.* International Journal of Heat and Mass Transfer, 1991. **34**(12): p. 3083-3095.

Ozdemir, M., *An experimental study on an oscillating loop heat pipe consisting of three interconnected columns.* Heat and Mass Transfer, 2007. **43**(6): p. 527-534.

Ramesh, P. and K. Torrance, *Stability of boiling in porous media.* International journal of heat and mass transfer, 1990. **33**(9): p. 1895-1908.

Rannenberg, M. and H. Beer, *Heat transfer by evaporation in capillary porous wire mesh structures.* Letters in Heat and Mass Transfer, 1980. **7**(6): p. 425-436.

Rudemiller, G.R., *A fundamental study of boiling heat transfer mechanisms related to impulse drying.* 1989.

Sondergeld, C.H. and D. Turcotte, *An experimental study of two-phase convection in a porous medium with applications to geological problems.* Journal of Geophysical Research, 1977. **82**(14): p. 2045-2053.

Udell, K.S., *Heat transfer in porous media considering phase change and capillarity—the heat pipe effect.* International Journal of Heat and Mass Transfer, 1985. **28**(2): p. 485-495.

Xiaoguo, T. and P. Cheng, *Correlations of the cycle-averaged Nusselt number in a periodically reversing pipe flow.* International Communications in Heat and Mass Transfer, 1993. **20**(2): p. 161-172

Wan, Z.P., X.W. Wang, and Y. Tang, *Condenser design optimization and operation characteristics of a novel miniature loop heat pipe.* Energy Conversion and Management, 2012. **64**: p. 35-42

Wang, X.W., Z.P. Wan, and Y. Tang, *Heat transfer mechanism of miniature loop heat pipe with water-copper nanofluid: thermodynamics model and experimental study.* Heat and Mass Transfer, 2013. **49**(7): p. 1001-1007.

Watson, E.J., *Diffusion in Oscillatory Pipe-Flow.* Journal of Fluid Mechanics, 1983. **133**(Aug): p. 233-244.

Zhang, J.G. and U.H. Kurzeg, *Numerical simulation of time-dependent heat transfer in oscillating pipe flow.* Journal of Thermophysics and Heat Transfer, 1991. **5**(3): p. 401-406.

Zhao, T.S. and P. Cheng, *A numerical study of laminar reciprocating flow in a pipe of finite length.* Applied Scientific Research, 1998. **59**(1): p. 11-25.

Zhao, T. and P. Cheng, *A Numerical-Solution of Laminar Forced-Convection in a Heated Pipe Subjected to a Reciprocating Flow.* International Journal of Heat and Mass Transfer, 1995. **38**(16): p. 3011-3022.

Zhao, T.S. and P. Cheng, *Oscillatory Heat Transfer in a Pipe Subjected to a Laminar Reciprocating Flow.* Journal of Heat Transfer, 1996. **118**(3): p. 592-597